

Mono- and Heterodimetallic Fe^{II} and Ru^{II} Complexes Based on a Novel Heteroditopic 4'-{Bis(phosphanyl)aryl}-2,2':6',2''-terpyridine Ligand

Marcella Gagliardo,^[a] Jolke Perelaer,^[a] František Hartl,^[b] Gerard P. M. van Klink,^[a] and Gerard van Koten*^[a]

Keywords: Ruthenium / Iron / Terpyridine ligands / Pincer ligands / Spectroelectrochemistry

In the search for a versatile building block that allows the preparation of heteroditopic tpy-pincer bridging ligands, the synthon {4'-[C₆H₃(CH₂Br)₂-3,5]-2,2':6',2''-terpyridine} was synthesized. Facile introduction of diphenylphosphanyl groups in this synthon gave the ligand {4'-[C₆H₃(CH₂-PPh₂)₂-3,5]-2,2':6',2''-terpyridine} ([**tpyPC(H)P**]). The asymmetric mononuclear complex [Fe(tpy){**tpyPC(H)P**]}(PF₆)₂, prepared by selective coordination of [Fe(tpy)Cl₃] to the tpy moiety of [**tpyPC(H)P**], was used for the synthesis of the heterodimetallic complex [Fe(tpy)(**tpyPCP**)Ru(tpy)](PF₆)₃, which applies the "complex as ligand" approach. Coordination of the ruthenium centre at the PC(H)P-pincer moiety of [Fe(tpy){**tpyPC(H)P**]}(PF₆)₂ has been achieved by applying a transcyclometallation procedure. The ground-state electronic

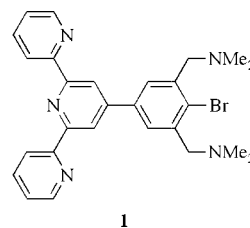
properties of both complexes, investigated by cyclic and square-wave voltammetries and UV/Vis spectroscopy, are discussed and compared with those of [Fe(tpy)₂](PF₆)₂ and [Ru(PCP)(tpy)]Cl, which represent the mononuclear components of the heterodinuclear species. An in situ UV/Vis spectroelectrochemical study was performed in order to localize the oxidation and reduction steps and to gain information about the Fe^{II}-Ru^{II} communication in the heterodimetallic system [Fe(tpy)(**tpyPCP**)Ru(tpy)](PF₆)₃ mediated by the bridging ligand [**tpyPCP**]. Both the voltammetric and spectroelectrochemical results point to only very limited electronic interaction between the metal centres in the ground state. © Wiley-VCH Verlag GmbH & Co. KGaA, 69451 Weinheim, Germany, 2007)

Introduction

In the past decades, much attention was devoted to the field of coordination chemistry of substituted terpyridines. Currently, a significant amount of research is devoted to the preparation of mononuclear terpyridine complexes bearing an externally oriented vacant binding site. A huge potential is concealed in these compounds with tuneable redox and photophysical properties, which can be used as building blocks for the construction of molecular devices,^[1] metal-containing dendrimers^[2] and one-dimensional polymers.^[3]

Only a few examples have been reported in which metal-tpy and organometallic subunits are incorporated into a single molecule.^[4] Bridging ligands based on 2,2':6',2''-terpyridine (tpy) functionalized at the 4'-position with a cyclometallating unit proved to have a high potential for linking chromophoric Ru-tpy centres and robust organometallic units containing a stable M-C σ-bond.^[1b,5] Recently, we described the synthesis of the heteroditopic ligand 4'-{4-Br-

C₆H₃(CH₂NMe₂)₂-3,5}-2,2':6',2''-terpyridine [**tpyNCNBr** (**1**)], which combines the properties of the tpy and NCNBr-pincer {BrC₆H₃(CH₂NMe₂)-2,6} ligands.^[6] It was shown that selective metallation and coordination of the NCNBr and tpy moieties, respectively, affords monometallic species that can be further used as building blocks for the construction of heterodi- and trimetallic complexes containing covalently linked photosensitizing octahedral [Ru(tpy)₂]²⁺ and cyclometalated NCN-Pd^{II} domains.^[6]



1

Metallation of the NCNBr moiety in **1** can be performed only by oxidative addition of the C-Br bond to transition-metal salts.^[7] For a broader application in template-directed synthesis of multimetallic systems based on metal-tpy binding domains containing aryl pincer components, we extended our studies to the preparation of the versatile tpy-pincer building block 4'-{C₆H₃(CH₂Br)₂-3,5}-2,2':6',2''-terpyridine (**5**). Interestingly, **5** can be used as a precursor for several tpy-pincer ligand systems because the bromo

[a] Faculty of Science, Organic Chemistry and Catalysis, University of Utrecht, Padualaan 8, 3584 CH Utrecht, The Netherlands
Fax: +31-30-252-3615
E-mail: g.vankoten@chem.uu.nl

[b] Van't Hoff Institute for Molecular Sciences, Homogeneous and Supramolecular Catalysis, University of Amsterdam, Nieuwe Achtergracht 166, 1018 WV Amsterdam, The Netherlands

substituents at the benzylic arms can be easily converted into ER₂ groups, where E = N, P, S, O and R = alkyl or aryl.^[8] In the pincer moiety, several parameters (e.g. nature of the donor atoms, size and electron-withdrawing or releasing character of the donor substituents) can readily be varied. This allows for fine-tuning of the target ligand depending on its envisaged application.^[9] Moreover, incorporation of a wider range of transition metals into the pincer moiety can at the same time be achieved through C–H activation,^[10] transmetallation^[11] and transcyclometallation^[12] procedures.

In our previous work, we described a heterometallic system with weak electronic interactions between the Ru^{II} and Pd^{II} centres mediated by tpy-pincer ligand **1**.^[6] However, this study was hampered by the low redox activity of the Pd^{II} centre and by the instability of the NCN–Pd pincer moiety upon electrochemical reduction.^[6] Aimed at continuing these physicochemical investigations and with synthon **5** in hand, we focused our attention on its derivatization to form the heteroditopic ligand 4'-{C₆H₃(CH₂PPh₂)₂-3,5}-2,2':6',2''-terpyridine [{**tpyPC(H)P**] (**7**), see Scheme 1} containing P-donor atoms. Facile attachment of redox active Fe^{II} and Ru^{II} centres to the tpy and PCP-pincer moieties of **7**, respectively, led to the formation of the heterodimetallic complex [Fe(tpy)(**tpyPCP**)Ru(tpy)](PF₆)₃ (**11**). For the purpose of comparison, the mononuclear complex [Fe(tpy){**tpyPC(H)P**}]PF₆ (**9**) was also prepared. Our main goal was to investigate the spectroelectrochemical behaviour of **11** and the known reference complexes [Fe(tpy)₂]²⁺^[13] and [Ru(PCP)(tpy)]Cl (PCP = [C₆H₃(CH₂-

PPh₂)₂-2,6-]^[14] to probe the degree of intramolecular electronic interaction between the metal centres in the novel dinuclear species mediated by the **tpyPCP** bridging ligand.

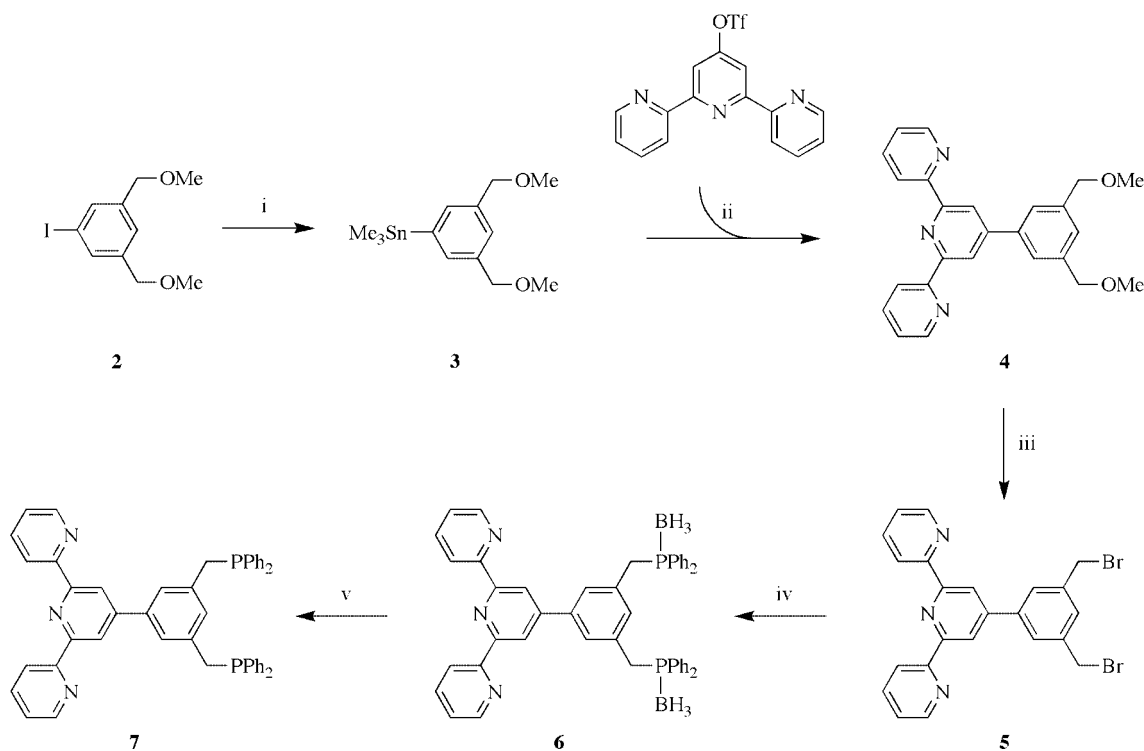
Results and Discussion

Synthesis of the [tpyPC(H)P] Ligand

The starting point for the synthesis of the building block 4'-{C₆H₃(CH₂Br)₂-3,5}-2,2':6',2''-terpyridine (**5**) (Scheme 1) is the preparation of the stannane pincer compound {C₆H₃(CH₂OMe)₂-3,5}-SnMe₃ (**3**). Chemoselective lithiation of 3,5-bis(methoxymethyl)iodobenzene **2**^[15] at the C–I position was achieved by reaction of **2** with 2 equiv. of *t*BuLi in Et₂O at –100 °C. Subsequent quenching with Me₃SnCl followed by slow warming of the reaction mixture to room temperature resulted in the formation of **3** in good yield. Pd-catalyzed Stille cross-coupling^[16] of **3** with 4'-triflate-2,2':6',2''-terpyridine^[17] gave **4** in moderate yield after chromatographic purification.

First attempts to replace the methoxy groups in **4** with bromide substituents by using BF₃·EtO₂/AcBr in CH₂Cl₂^[18] mainly resulted in the formation of unwanted side products and only small amounts of **5**. However, **5** was conveniently prepared by treatment of **4** with an excess amount of HBr·AcOH in dichloromethane.

Subsequently, a two-step procedure was employed for the preparation of **7**. First, treatment of **5** with 2 equiv. of in situ prepared LiPPh₂·BH₃ afforded **6**. Deprotection of the diphenylphosphine–BH₃ moieties with Et₂NH yielded **7** as



Scheme 1. Synthesis of [**tpyPC(H)P**] ligand **7**. Reagents and conditions: i) (a) 2 equiv. *t*BuLi, Et₂O, –100 °C, 0.5 h. (b) Me₃SnCl, Et₂O, –100 °C → room temp., 15 h. ii) LiCl, [PdCl₂(PPh₃)₂], toluene, reflux, 20 h. iii) (a) HBr·AcOH, CH₂Cl₂, room temp., 15 h. (b) aq. NaHCO₃. iv) HPPH₂·BH₃, *n*BuLi, THF, –78 °C → room temp., 20 h. v) (a) Et₂NH, room temp., 2 h. (b) aq. NaHCO₃.

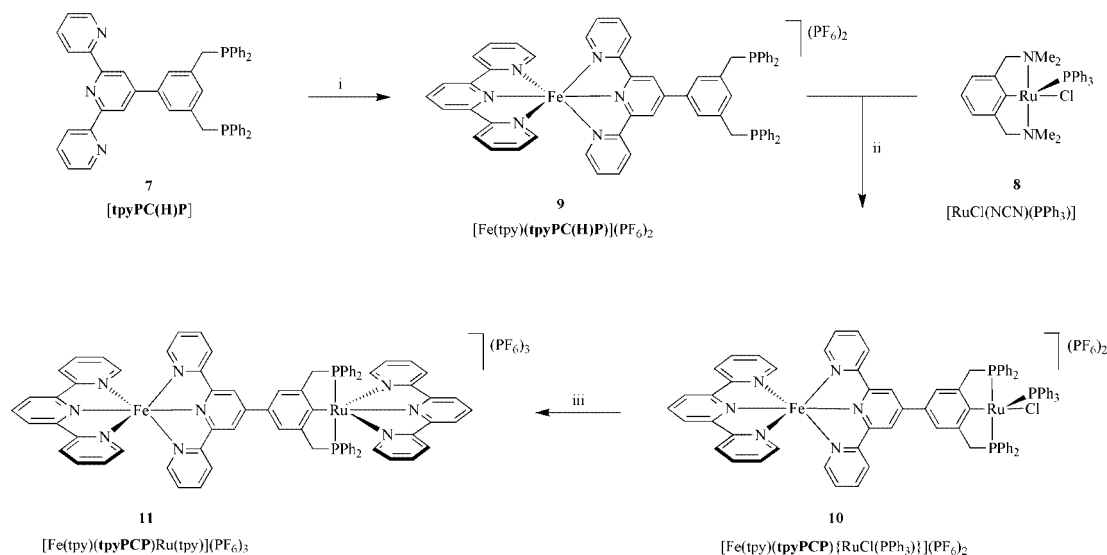
an air- and moisture-sensitive sticky white solid. Notably, both the tpy and PCP-pincer moieties of **7** proved to be stable both in acidic and basic media during the entire synthetic procedure. All the intermediates and ligand **7** have been fully characterized by analytical and spectroscopic methods. The ¹H and ¹³C NMR spectra of **7** show the characteristic coupling between the benzylic proton and carbon atoms, of the PPh₂ groups, respectively. The ³¹P{¹H} NMR spectrum exhibits a signal at $\delta = -8.5$ ppm typical for the diphenylphosphanyl groups.

Syntheses of Mono- and Heterodimetallic Complexes

Previous work carried out by Constable and co-workers^[19] showed the high potential of the phosphane-functionalized terpyridine ligand 4'-(PPh₂)-2,2':6',2''-terpyridine to link M^{II} coordination centres (M = Fe, Ru) and organometallic units through the N,N,N- and P-donor domains, respectively. Because it was demonstrated that reaction of ruthenium(III) chloro complexes with this ligand leads to partial or complete oxidation of the PPh₂ group,^[19a] it was decided to employ different ruthenium starting materials to produce the (tpyPCP)Ru-containing species. The use of [RuCl₂(PPh₃)₃] gave a mixture of N,N,N- and P-bound compounds. Confident that a selective and quantitative transfer of the RuClPPh₃-moiety into the PCP-pincer unit of **7** could be achieved by a transcyclometallation (TCM) procedure developed in our laboratories for the synthesis of multi(pincer-metal) complexes,^[12,20] we reacted the ruthenium precursor [RuCl(NCN)(PPh₃)]^[21] (NCN = [C₆H₃(CH₂NMe₂)₂-2,6]⁻) (**8**, Scheme 2) with **7** in refluxing benzene. Resonances of free **7** or unreacted **8** (singlet at $\delta = 90.2$ ppm) were subsequently not detected in the ³¹P{¹H} NMR spectrum. The main signals present in the spectrum, a triplet at $\delta = 83.2$ ppm (PPh₃, ²J_{PP} = 31.8 Hz) and a doublet at $\delta = 37.9$ ppm (PCP, ²J_{PP} = 31.8 Hz), together with a

large amount of free PPh₃, are consistent with the incorporation of the ruthenium centre into the PCP-pincer unit by TCM.^[12a] However, the presence of a singlet at $\delta = 41.82$ ppm indicated that an unwanted reaction concomitant to the TCM procedure occurred. The ruthenium centre of the {(PCP)RuCl(PPh₃)} moiety partly reacted with the tpy site of another molecule of the bridging ligand, which produced an oligonuclear species containing the unit [(PCP)Ru(tpyPCP)RuCl(PPh₃)]. The nature of this material was not investigated in detail. However, fine-tuning of the reaction conditions, as well as the introduction of solubilizing substituents at the phosphorus atoms, may give rise to the formation of soluble redox- and photoactive organometallic molecular wires. Because the synthesis of mononuclear complexes incorporating **7** failed as a result of the affinity of both PCP-pincer and tpy sites for ruthenium, we decided to choose a different approach: to first coordinate an iron centre to the tpy unit in **7**, and then to bind the ruthenium centre at the PCP-site through a TCM reaction.

The reaction of equivalent amounts of [Fe(tpy)Cl₃]^[22] and **7** in refluxing methanol resulted in the formation of an intensely purple-coloured solution, from which the cation [Fe{tpyPC(H)P}(tpy)]²⁺ could be isolated as the diamagnetic PF₆-salt **9** (Scheme 2). Similarly to what was found for **7**, complex **9** is highly air and moisture-sensitive and has to be handled under strictly anaerobic conditions. This sensitivity hampered the removal of small amounts of tpy-containing impurities by chromatography. Attempts to obtain single-crystals suitable for X-ray diffraction analysis were, unfortunately, also unsuccessful. However, complex **9** was sufficiently characterized by NMR spectroscopy and high-resolution ESI-MS analysis. In the ESI-MS spectrum of **9**, the highest mass peak at $m/z = 497.20$ corresponds to [M - 2 PF₆]²⁺, which shows the correct isotopic pattern for this formulation. The resonances in the aromatic region of the ¹H NMR spectrum could be unequivocally assigned to the protons of the complexed tpy moieties. A single resonance



Scheme 2. Synthesis of **9** and heterodimetallic **11**. Reagents and conditions: i) (a) 1 equiv. [Fe(tpy)Cl₃], MeOH, reflux, 4 h. (b) Excess NH₄PF₆. ii) **8**, THF/MeCN, reflux, 2 d. iii) (a) tpy, MeOH. (b) Excess NH₄PF₆.

in the $^{31}\text{P}\{^1\text{H}\}$ NMR spectrum ($\delta = -4.9$ ppm in CD_3CN) for the equivalent diphenylphosphanyl groups clearly indicates that the iron centre is selectively coordinated to the tpy moiety.

Ruthenation of the PCP-pincer unit of **9** was achieved by the TCM procedure: the reaction of **9** with an equivalent amount of **8** in refluxing THF/MeCN (8:3 v/v). Removal of the volatiles gave intermediate species **10** (Scheme 2) that was subsequently treated with tpy in refluxing methanol. Addition of aqueous NH_4PF_6 to the red–purple methanolic solution resulted in the precipitation of **11** as a wine-red solid.

The presence of the PPH_2 groups and three nonequivalent tpy ligands results in a complicated ^1H NMR spectrum in the aromatic region. Nevertheless, the resonances of **11** could be assigned by comparison with the data obtained for **9** and $[\text{Ru}(\text{PCP})(\text{tpy})]\text{Cl}$.^[14] The ^1H and $^{31}\text{P}\{^1\text{H}\}$ NMR spectra reveal a high degree of symmetry for the $\{(\text{PCP})\text{-Ru}(\text{tpy})\}$ unit in **11**, with the geometry in solution probably very close to that of $[\text{Ru}(\text{PCP})(\text{tpy})]\text{Cl}$. The aliphatic region of the ^1H NMR spectrum shows a singlet resonance for the equivalent benzylic hydrogens, which is indicative of a molecular mirror plane containing the benzylic carbon atoms. These data, together with the peak at $\delta = 41.82$ ppm in the $^{31}\text{P}\{^1\text{H}\}$ NMR spectrum for the equivalent phosphorus nuclei, suggest an octahedral geometry of the ruthenium coordination sphere, with both the PCP-pincer and tpy ligands coordinated in a meridional fashion. The ESI-MS spectrum of **11** displays $[\text{M} - 3\text{PF}_6]^{3+}$ ($m/z = 442.75$) and $[\text{M} - 2\text{PF}_6]^{2+}$ ($m/z = 736.67$) for the heterodinuclear complex with good isotopic matching to the simulated spectrum.

Redox Behaviour and Electronic Absorption Spectra

The electrochemical and spectroscopic properties of the prepared compounds were studied with the aim to estimate the extent of the $\text{Fe}^{\text{II}}\text{-Ru}^{\text{II}}$ interactions within **11**, mediated by bridging ligand **7**. The redox behaviour of **9** and **11** was investigated by cyclic and square-wave voltammetries (CV and SWV) in MeCN at room temperature. Pertinent electrochemical data are collected in Table 1. Literature data for $[\text{Fe}(\text{tpy})_2](\text{PF}_6)_2$ ^[13] and $[\text{Ru}(\text{PCP})(\text{tpy})]\text{Cl}$ ^[14] have been included for reference purposes.

Table 1. Electrochemical data for complexes **9** and **11**, and reference compounds.^[a]

Complex	$E_{1/2}$ [V] (oxidation)	$E_{1/2}$ [V] (reduction)
$[\text{Fe}(\text{tpy})_2](\text{PF}_6)_2$ ^[b]	0.74	-1.64, -1.82
$[\text{Ru}(\text{PCP})(\text{tpy})]\text{Cl}$ ^[c]	0.17	-1.95
$[\text{Fe}(\text{tpy})\{\text{tpyPC}(\text{HPP})\}](\text{PF}_6)_2$ (9)	0.74	-1.59; -1.69
$[\text{Fe}(\text{tpy})(\text{tpyPCP})\text{Ru}(\text{tpy})](\text{PF}_6)_3$ (11)	0.16	-1.93
	0.71	-1.62; -1.77

[a] Measured in MeCN containing 10^{-1} M TBAH at 298 K. Electrode potentials are given in Volt versus Fc/Fc^+ . Scan rate = 100 mV s^{-1} . [b] Ref.^[13] [c] Ref.^[14]

It is well known that redox processes for common $\text{Ru}^{\text{II}}\text{-}$ polypyridine complexes are mainly localized either on the

metal centres (oxidations) or the ligands (reductions).^[23] According to experimental results previously reported,^[13a,13b] oxidation of the $\text{Fe}^{\text{II}}\text{-tpy}$ complexes can be assigned as metal-localized.^[13c] However, DFT calculations performed on the complexes $[\text{Fe}(\text{tpy})_2]^{2+}$ and $[\text{Fe}(\text{B-tpy})_2]^{2+}$ {B-tpy = 4'-(*tert*-butyl-phenyl)-2,2':6',2''-terpyridine} showed that the highest molecular orbital (HOMO) of these compounds is not solely iron-based.^[13c] In fact, the HOMO of the complex $[\text{Fe}(\text{tpy})_2]^{2+}$ resides mainly on one of the tpy ligands and partly on the iron. Introduction of a substituted phenyl group at the 4'-position of the terpyridine ligands in $[\text{Fe}(\text{B-tpy})_2]^{2+}$ significantly changes the HOMO character relative to that of $[\text{Fe}(\text{tpy})_2]^{2+}$, which has a stronger metal $d\pi$ component, with a contribution from the phenyl π orbitals.^[13c] The lowest unoccupied molecular orbital (LUMO) of $[\text{Fe}(\text{tpy})_2]^{2+}$ is localized on both tpy ligands, whereas the LUMO of $[\text{Fe}(\text{B-tpy})_2]^{2+}$ is mainly localized on only one of the B-tpy ligands and partly on the metal.^[13c]

The redox potentials determined for **9** and **11** are close to those reported for other $\text{Fe}^{\text{II}}\text{-tpy}$ complexes (Table 1). This indicates that the oxidation and reduction of these species involve frontier orbitals having comparable energy and probably also similar character to those calculated for $[\text{Fe}(\text{B-tpy})_2]^{2+}$. Thus, the reversible anodic wave at $E_{1/2} = 0.74$ V ($\Delta E_p = 0.60$ mV) in the cyclic voltammogram of **9** corresponds to a one-electron oxidation of the $\text{Fe}^{\text{II}}\text{-tpy}$ moiety. In the cathodic region, two reversible one-electron waves at -1.59 V ($\Delta E_p = 0.58$ mV) and -1.69 V ($\Delta E_p = 0.54$ mV) belong to the sequential reduction of the tpy ligands. By comparison with $[\text{Fe}(\text{tpy})_2]^{2+}$,^[13b] we assign the first and second reduction steps in **9** to the pincer-substituted and terminal tpy ligands, respectively. The electron-withdrawing character of the phenyl moiety renders the substituted tpy less electron rich, thereby decreasing its reduction potential. The anodic potential region of the heterodinuclear complex **11** exhibits two reversible, one-electron anodic waves due to the Ru^{II} centre at $E_{1/2} = 0.16$ V ($\Delta E_p = 0.56$ mV) and the $\text{Fe}^{\text{II}}\text{-tpy}$ moiety at $E_{1/2} = 0.71$ V, respectively. These values are nearly identical with the electrode potentials of the $\text{Fe}^{\text{II}}\text{-tpy}$ and Ru^{II} -based oxidations of complex **9** and $[\text{Ru}(\text{PCP})(\text{tpy})]\text{Cl}$, respectively. Apparently, the electronic communication between the metal centres is very limited. In the cathodic region, complex **11** undergoes three ligand-centred reduction processes. The first two cathodic waves lie at -1.62 V and -1.77 V. The initial reduction is fully reversible ($\Delta E_p = 0.54$ mV). The second cathodic step, however, is characterized by slower electron transfer as indicated by decreased peak currents in both voltammetric (CV and SWV) records. More information about this behaviour has been obtained from the corresponding spectroelectrochemical experiments (see below). According to the reference data in Table 1, these reductions are localized at the terminal and substituted tpy ligands that are coordinated to the iron centre, respectively. The third cathodic step at -1.92 V ($\Delta E_p = 0.60$ mV), which is fully reversible, can be readily assigned to the reduction of the terminal tpy ligand bound to the ruthenium centre. The reduction

potential is only slightly less negative than that of the tpy ligand in [Ru(PCP)(tpy)]Cl (Table 1). These observations are consistent with a negligible electronic communication between the Ru(tpy) and the doubly reduced (tpy)Fe-(**tpyPCP**) moieties.

The electronic absorption spectra of **9** and **11** were recorded in MeCN solution at room temperature. Absorption maxima (λ_{max}) and molar absorption coefficients (ϵ_{max}) for both compounds are listed in Table 2, together with the reference data for [Fe(tpy)₂](PF₆)₂^[13] and [Ru(PCP)(tpy)]Cl.^[14] The UV/Vis spectra of **9** and **11** show features typical for other Fe^{II}- and Ru^{II}-tpy compounds,^[13,23] in particular intense $\pi \rightarrow \pi^*$ intraligand (IL) transitions in the UV region, 320 and 280 nm for **9**, and at 308, 319 and 275 nm for **11**. In the visible spectral region, complexes **9** and **11** exhibit moderately intense visible absorption bands (Figure 1) that are tentatively attributed to electronic transitions having a mixed $\pi(\text{tpy}) \rightarrow \pi^*(\text{tpy})$ IL and $d\pi(\text{Ru}) \rightarrow \pi^*(\text{ph})$ MLCT character by comparison with literature data on the basis of the TD-DFT calculations performed on the complexes [Fe(tpy)₂]²⁺ and [Fe(B-ptpy)₂]²⁺ (B-ptpy = 4'-(*n*-butylphenyl)-2,2':6',2''-terpyridine) (vide supra).^[13c,23] The small shift in the lowest absorption of **9** and **11** (Figure 1) to a lower energy relative to [Fe(tpy)₂](PF₆)₂ is consistent with the electrochemical results. The lowest transition of **9** is only slightly affected by the incorporation of the ruthenium centre into the PCP-pincer unit (Table 2).

Table 2. UV/Vis absorption maxima (λ_{max}) and molar absorption coefficients (ϵ_{max}) of complexes **9** and **11**, and reference compounds.^[a]

Compound	λ_{max} [nm] ($\epsilon_{\text{max}} \cdot 10^{-4}$ [M ⁻¹ cm ⁻¹])
[Fe(tpy) ₂](PF ₆) ₂ ^[b]	548 (1.4)
[Ru(PCP)(tpy)]Cl ^[c]	275 (3.7), 305 (3.9), 479 (0.8)
[Fe(tpy) ₂](tpyPC(H)P)(PF ₆) ₂ (9)	280 (5.9), 320 (5.6), 563 (1.0)
[Fe(tpy)(tpyPCP)Ru(tpy)](PF ₆) ₃ (11)	275 (5.1), 308 (4.1), 319 (4.0), 489 (0.8), 563 (1.0)

[a] Measured at 298 K in MeCN. [b] Ref.^[13] [c] Ref.^[14]

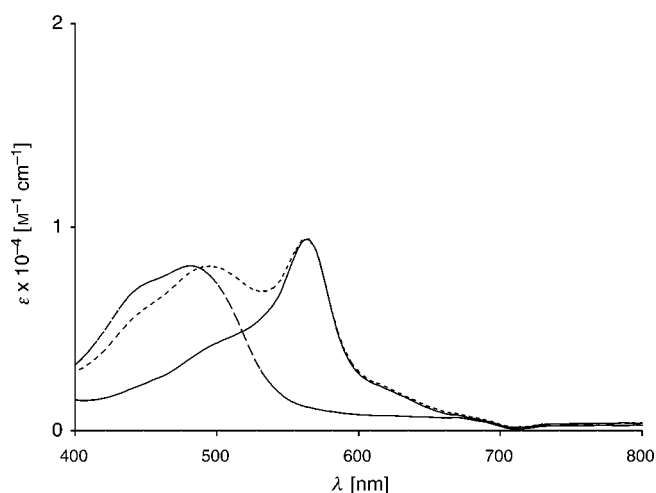


Figure 1. Visible region of the absorption spectra of complexes [Ru(PCP)(tpy)]Cl (---), **9** (—), and **11** (.....) recorded in MeCN at 298 K.

For the ruthenium centre in [Ru(PCP)(tpy)]Cl, it is expected that the lowest MLCT excited state involves the coordinated tpy ligands rather than the strongly donating cyclometallated PCP-pincer ligand.^[14] The Ru-to-tpy CT band of complex **11** at 489 nm is only slightly shifted to a lower energy relative to the mononuclear [Ru(PCP)(tpy)]Cl (Table 2). This shift, although small, is in agreement with the less positive oxidation and less negative reduction potentials of the Ru(tpy) moiety in the latter complex (Table 1), that is, with a slightly larger HOMO – LUMO gap: $\Delta E = 0.03$ eV. These results again reveal that the electronic communication between the **tpyPCP**-bridged Ru(tpy) and Fe(tpy) moieties in complex **11** is very limited. A large dihedral angle between the tpy and the PCP-pincer units of the bridging ligand is the most likely reason for the lack of electronic coupling between the two motifs.^[24]

However, it cannot be excluded that stabilization of the ruthenium orbitals by π -back donation to the PPh₂ moieties to some extent contributes to a decrease in the mixing between the $d\pi(\text{Ru})$ - and the bridging ligand-based orbitals, and thus, the metal-coupling in the studied heterodimetallic complex.

UV/Vis Spectroelectrochemistry

UV/Vis spectroelectrochemical studies of heterodimetallic complex **11** were performed in MeCN at room temperature within an optically-transparent thin-layer electrochemical (OTTLE)^[25] cell. These investigations were mainly aimed at gaining more information about the degree of the Fe^{II}-Ru^{II} interaction mediated by the twisted bridging ligand [**tpy(PCP)**]. In addition, the spectral changes recorded during the oxidation and reduction steps help to more accurately appoint their assignment in the preceding section.

Electrochemical oxidation of **11** to **11**⁺ at 0.16 V caused flattening of the band at 500 nm (Figure 2), consistent with

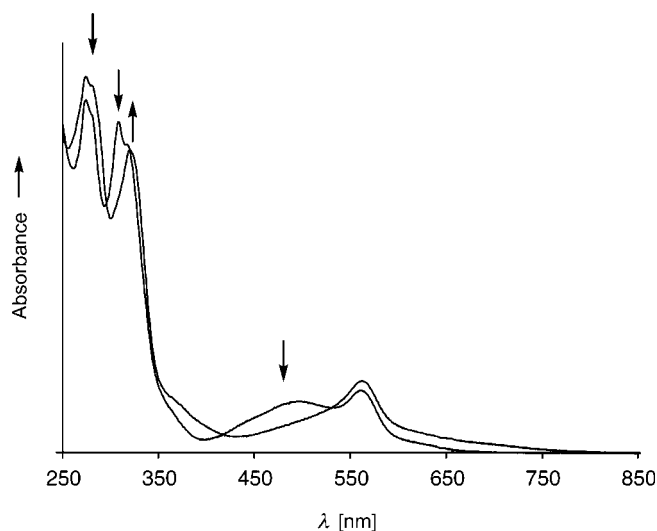


Figure 2. UV/Vis spectra recorded during one-electron oxidation of the Ru^{II} centre in complex **11**. Conditions: OTTLE cell, MeCN/10⁻¹ M TBAH, 293 K.

its assignment to the MLCT transition in the {Ru(tpy)} moiety. Further oxidation of $\mathbf{11}^+$ to $\mathbf{11}^{2+}$ at 0.70 V then resulted in disappearance of the composed absorption band at 565 nm (Figure 3), which agrees with the oxidation of the Fe(tpy) moiety. The formation of $\mathbf{11}^+$ and $\mathbf{11}^{2+}$ is also accompanied by stepwise disappearance of the $\pi \rightarrow \pi^*$ absorption bands at 308 and 319 nm, respectively. Accordingly, they can be attributed to intraligand Ru(tpy) and Fe(tpy) transitions, respectively. This assignment, supported also by the reference data ([Ru(PCP)(tpy)]Cl and complex **9** in Table 2), is also important for the discussion of the cathodic steps (see below). Reduction of $\mathbf{11}^{2+}$ at 0.16 V led to full recovery of the electronic absorption spectrum of **11**.

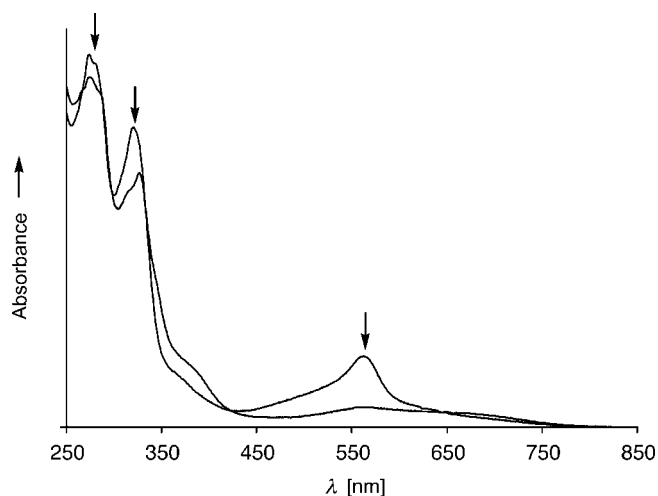


Figure 3. UV/Vis spectra recorded during one-electron oxidation of complex $\mathbf{11}^+$, which is probably localized at the Fe(tpy) moiety.^[13c] The preceding anodic step is depicted in Figure 2. Conditions: OTTLE cell, MeCN/ 10^{-1} M TBAH, 293 K.

The spectroscopic changes observed during one-electron reduction of the heterodinuclear complex **11** to $\mathbf{11}^-$ were very similar to those observed in the UV/Vis spectra of the singly and doubly reduced complex $[\text{Fe}(\text{tpy})_2]^{2+}$.^[13b] Reduction of **11** at -1.73 V led to the disappearance of the mixed IL/MLCT band at 565 nm (Figure 4). New low-lying absorption bands due to $\pi^* \rightarrow \pi^*(\text{tpy}^-)$ transitions^[13b] arose at 641, 736 and 905 nm (Figure 4). The persisting Ru-to-tpy CT transition of $\mathbf{11}^-$ at 498 nm, as well as the unaffected intraligand Ru(tpy) transition at 308 nm also prove that the first reduction step is localized on the terminal tpy ligand coordinated at the iron(II) centre. The slightly decreased intensity of the band at 498 nm in the UV/Vis spectrum of $\mathbf{11}^-$ is most probably caused by the disappearance of the underlying shoulder of the composed IL/MLCT Fe(tpy)-band (Figure 1).^[13c] Unlike that reported for $[\text{Fe}(\text{tpy})_2]^{2+}$,^[13b] the addition of the second electron did not result in a shift of the $\pi^* \rightarrow \pi^*(\text{tpy}^-)$ transitions to lower energies. Instead, the formation of $\mathbf{11}^{2-}$ resulted in the increasing intensity of the broad $\pi^* \rightarrow \pi^*$ absorption between 550–900 nm, with the main absorption maximum at 732 nm (Figure 4).

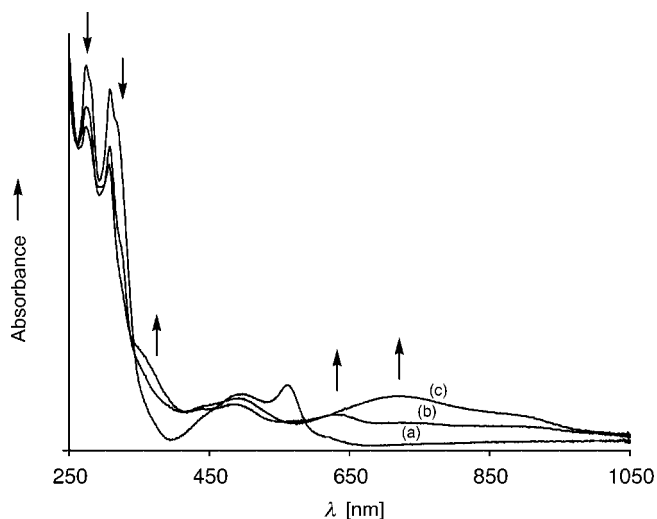


Figure 4. UV/Vis spectral changes accompanying reduction of complex **11** (a) to $\mathbf{11}^-$ (b) and $\mathbf{11}^{2-}$ (c) in two tpy(Fe)-localized steps. Conditions: OTTLE cell, MeCN/ 10^{-1} M TBAH, 293 K.

Importantly, the Ru-to-tpy CT and $\pi \rightarrow \pi^*$ Ru(tpy) bands also do not change during the second cathodic step, which indicates that this step is localized on the substituted tpy part of the bridging [tpyPCP] ligand. These findings again reveal only a weak communication between the two metal centres through the tpyPCP bridge. The qualitatively different changes in the visible spectral region upon the formation of $\mathbf{11}^{2-}$ compared with the doubly reduced reference $[\text{Fe}(\text{tpy})_2]^{13b}$ may reflect some involvement of the phenyl ring of the pincer part of the bridging ligand in the occupied π^* system, possibly due to some variation in the central twist angle caused by the second reduction. This observation may explain the slower voltammetric response to the second electron transfer than the first, electrochemically reversible cathodic step of **11**. The third one-electron reduction producing $\mathbf{11}^{3-}$ caused flattening of the Ru-to-tpy CT band. The $\pi \rightarrow \pi^*$ Ru(tpy) absorption band at 308 nm

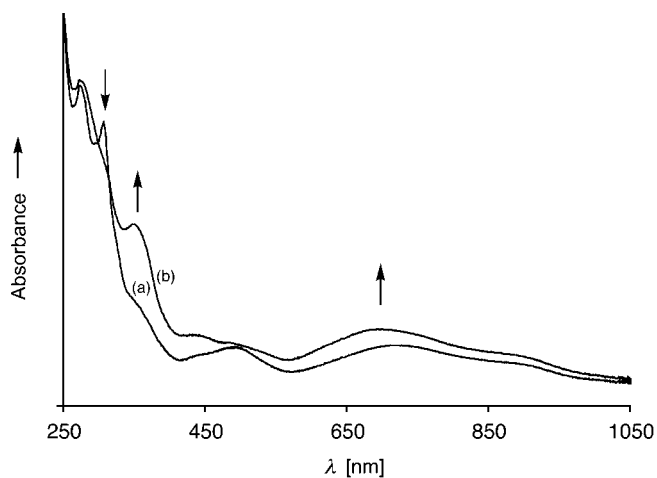


Figure 5. UV/Vis spectrum of $\mathbf{11}^{3-}$ (b) formed from $\mathbf{11}^{2-}$ (a) in the third, tpy(Ru)-localized cathodic step. Conditions: OTTLE cell, MeCN/ 10^{-1} M TBAH, 293 K.

also became affected (Figure 5). Importantly, a new $\pi^* \rightarrow \pi^*(\text{tpy}^-)$ absorption appeared around 550 nm.

Similar spectral changes are characteristic for the one-electron reduction of the reference complex [Ru(PCP)(tpy)]Cl (Figure 6), which confirms that the third reduction step of complex **11** involves occupation of the lowest π^* orbital that is essentially localized on the Ru-bound terminal terpyridine ligand, tpy(Ru).

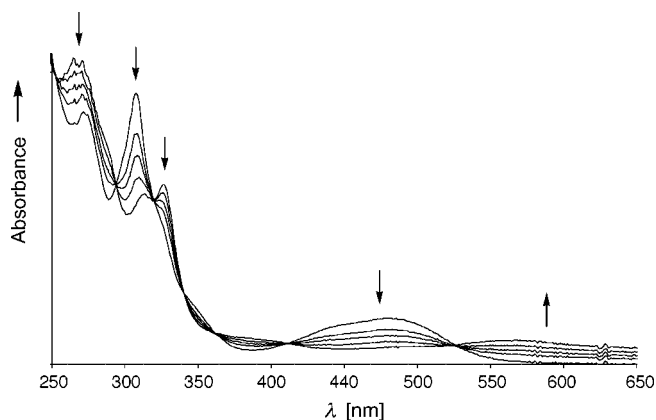


Figure 6. UV/Vis spectral changes accompanying the tpy-localized one-electron reduction of the reference complex [Ru(PCP)(tpy)]Cl. Conditions: OTTLE cell, MeCN/ 10^{-1} M TBAH, 293 K.

Reoxidation of all three one-electron-reduced species, $\mathbf{11}^{n-}$ ($n = 1, 2, 3$), fully regenerated the UV/Vis spectrum of parent **11**. It is clear that the reduction steps are largely tpy-localized. The stability of the Ru–C σ -bond during the second and third cathodic steps is remarkable and is a consequence of this localization. In fact, significant delocalization of the added electron density over the PCP-pincer moiety would most likely break the Ru–C σ -bond.^[6]

Conclusions

In this work, the synthesis of novel building block 4'-{C₆H₃(CH₂Br)₂-3,5}-2,2':6',2''-terpyridine is presented, which can be used as a precursor for bridging ligands containing an N,N,N-domain and an E,C,E-coordination (E = N, P, S, O) motive. Heteroditopic tpy-pincer ligands are interesting from different viewpoints. In particular, electronic and steric properties of the pincer moiety, in which several transition metals can be incorporated by applying various metallation procedures, can easily be tuned.

Incorporation of diphenylphosphanyl groups gave the 4'-{C₆H₃(CH₂PPh₂)₂-3,5}-2,2':6',2''-terpyridine [tpyPC(H)P] ligand. The asymmetric complex [Fe(tpy){tpyPC(H)P}](PF₆)₂, prepared by reaction of [tpyPC(H)P] with 1 equiv. of [Fe(tpy)Cl₃], was used for the construction of the heterodimetallic complex [Fe(tpy)(tpyPCP)Ru(tpy)](PF₆)₃, which follows the "complex as ligand" approach.

For both complexes, the oxidation and reduction processes have been assigned by comparison with literature data reported for related Fe^{II}-tpy compounds and with [Ru(PCP)(tpy)]Cl, which was extensively studied in this work. The redox potentials do not significantly change on

passing from the mononuclear Fe^{II} to the heterodimetallic Fe^{II}-Ru^{II} complex. UV/Vis spectroelectrochemical studies of the heterodimetallic complex confirm the voltammetric results. The spectral changes allow the stepwise Ru^{II}- and Fe^{II}-tpy oxidations to be distinguished. The first and second reduction steps are localized at the terminal and pincer-substituted tpy ligands coordinated at the iron centre, respectively. The third reduction resides at the tpy ligand coordinated at the ruthenium centre.

Apparently, despite the relatively moderate internuclear separation, only a very weak electronic interaction exists between the {Fe(tpy)₂} and {(PCP)Ru(tpy)} fragments. This can be rationalized in terms of the very limited ability of the nonplanar (twisted) [tpyPCP] bridging ligand to mediate electronic communication between the metal centres. However, stabilization of the $d\pi(\text{Ru})$ orbitals as a result of the π -accepting properties of the PPh₂ moieties may also cause a decrease in the Fe–Ru coupling by limiting the overlap between the ruthenium orbitals and the bridging ligand orbitals. Connection of the {Fe(tpy)₂} and {(PCP)Ru(tpy)} fragments through a bridge capable of achieving a more effective aromatic conjugation would be highly desirable.^[26]

Experimental Section

General: All experiments were carried out under a dry nitrogen atmosphere by using standard Schlenk techniques. Benzene, toluene, pentane, hexane and diethyl ether (Et₂O) were distilled from sodium/benzophenone. Dichloromethane and methanol were dried with CaH₂ and magnesium, respectively. All solvents were freshly distilled under a nitrogen atmosphere prior to use. 1D NMR spectra were recorded with a Varian Inova 300 MHz spectrometer. Chemical shifts are given in ppm relative to the residual solvent signal (¹H and ¹³C NMR spectra) or 85% H₃PO₄ external reference (³¹P{¹H} NMR spectra). EtOAc and all reagents were purchased from Acros or Aldrich and used as received. Compounds **2**,^[15] 4'-trifluoromethylsulfonato-2,2':6',2''-terpyridine,^[17] **8**^[21] and [Fe(tpy)Cl₃]^[22] were synthesized according to literature procedures. Elemental analyses were performed by Dornis und Kolbe, Mikroanalytisches Laboratorium, Mülheim a. d. Ruhr, Germany. Electron spray ionization (ESI) mass spectra were recorded with a Micromass LC-TOF mass spectrometer by the Department of Biomolecular Mass Spectrometry, Utrecht University.

Electrochemical Measurements: Cyclic and square-wave voltammetric scans were performed with a gas-tight single compartment cell under a dry nitrogen atmosphere. The cell was equipped with a Pt microdisk working electrode (apparent surface area of 0.42 mm²), Pt wire auxiliary electrode and a Ag wire pseudoreference electrode. The working electrode was carefully polished with a 0.25 μm -grain diamond paste between scans. The potential control was achieved with a PAR Model 283 potentiostat. All redox potentials are reported against the ferrocene-ferrocenium (Fc/Fc⁺) redox couple used as an internal standard^[27] ($E_{1/2} = +0.63$ V versus NHE^[28]). All electrochemical samples were 5×10^{-4} M in the studies complexes and 10^{-1} M in Bu₄NPF₆ used as the supporting electrolyte.

Electronic Spectroscopic Measurements: UV/Vis absorption spectra were obtained with a Varian Cary 1 spectrophotometer by using matched 1 cm cells and operating with a 0.5 nm spectral resolution. Peak positions are given within 0.5 nm accuracy.

UV/Vis Spectroelectrochemical Measurements: All the experiments were performed with an optically transparent thin-layer electrochemical (OTTLE)^[25] cell, equipped with a Pt minigrid working electrode and quartz optical windows. The controlled-potential electrolyses were carried out with a PA4 potentiostat (EKOM, Polná, Czech Republic). All electrochemical samples were 5×10^{-4} M in the studied complex and 10^{-1} M in Bu_4NPF_6 . UV/Vis spectra were recorded with a Hewlett Packard 8453 diode-array spectrophotometer.

[C₆H₃(CH₂OMe)₂-3,5]-SnMe₃ (3): A solution of *t*BuLi (13.0 mL, 1.5 M in pentane, 19.52 mmol) was added dropwise to a solution of **2** (3.00 g, 10.27 mmol) in Et₂O (75 mL) at -100 °C with vigorous stirring. After 0.5 h, a solution of Me₃SnCl (3.07 g, 15.41 mmol) in Et₂O (35 mL) was slowly added. The resulting pale yellow coloured suspension was warmed to room temperature and stirring was continued for another 15 h. Subsequently, water was added, and the obtained mixture was treated with a NaOH solution (0.1 M, 2×50 mL). The Et₂O layer was separated, and the water layer was washed with Et₂O (2×50 mL). The organic layers were combined, washed with brine, dried with MgSO₄, filtered and concentrated to afford **3** as a colourless oil. Yield: 2.95 g, 85%. ¹H NMR (300 MHz, CDCl₃): δ = 7.37 (s, 2 H, Ar), 7.26 (s, ²J_{Sn,H} = 21.7 Hz, 1 H, Ar), 4.43 (s, 4 H, OCH₂), 3.34 (s, 6 H, OCH₃), 0.29 [s, ²J_{Sn,H} = 27.0 Hz, 9 H, Sn(CH₃)₃] ppm. ¹³C NMR (75 MHz, CDCl₃): δ = 142.9 (¹J_{Sn,C} = 228.3 and 451 Hz), 137.9 (²J_{Sn,C} = 18.3 Hz), 134.7 (²J_{Sn,C} = 22.3 Hz, ArH), 127.5, 75.0 (OCH₃), 58.4 [CH₂, Sn(CH₃)₃], -9.3 [¹J_{Sn,C} = 171.5 Hz, Sn(CH₃)₃] ppm. ESI-MS: *m/z* 331.05 [M - H]⁺. C₁₃H₂₂O₂Sn (329.02): calcd. C 47.46, H 6.74; found C 47.55, H 6.62.

4'-[C₆H₃(CH₂OMe)₂-3,5]-2,2':6',2''-terpyridine (4): 4'-Trifluoromethylsulfonato-2,2':6',2''-terpyridine (2.66 g, 6.99 mmol), **3** (2.315 g, 6.99 mmol), [PdCl₂(PPh₃)₂] (0.41 g, 0.58 mmol) and dried LiCl (1.72 g, 40.6 mmol) were heated at reflux in dry toluene (100 mL) for 20 h in a 100-mL round-bottomed flask under a nitrogen atmosphere. Subsequently, the solvent was removed in vacuo, and the residue was redissolved in CH₂Cl₂. The CH₂Cl₂ solution was washed with water, filtered through Celite and dried with MgSO₄. The crude product was obtained as a light yellow oil after removal of the solvent as purified by silica gel column chromatography (EtOAc/MeOH 8:1). The fractions containing **4** were collected, concentrated and cooled to -30 °C. Product **4** precipitated as a white crystalline solid and was collected and dried in vacuo. Yield: 1.02 g, 40%. ¹H NMR (300 MHz, CDCl₃): δ = 8.75 [s, 2 H, tpy(3', 5')], 8.73 [d, J_{H,H} = 4.3 Hz, 2 H, tpyH(6, 6'')], 8.67 [d, J_{H,H} = 9.0 Hz, 2 H, tpyH(3, 3'')], 7.88 [td, J_{H,H} = 7.89, 1.61 Hz, 2 H, tpyH(4, 4'')], 7.80 (s, 2 H, ArH), 7.43 (s, 1 H, Ar), 7.35 [m, 2 H, tpyH(5, 5'')], 4.57 (s, 4 H, CH₂), 3.44 (s, 12 H, OCH₃) ppm. ¹³C NMR (75 MHz, CDCl₃): δ = 156.4, 156.0, 150.4, 149.2, 139.6, 139.0, 137.3, 127.8, 126.2, 124.0, 121.7, 119.3, 74.6 (OCH₃), 58.5 (CH₂) ppm. C₂₅H₂₃N₃O₂ (397.47): calcd. C 75.54, H 5.83, N 10.57; found C 75.63, H 5.88, N 10.62.

4'-[C₆H₃(CH₂Br)₂-3,5]-2,2':6',2''-tpy (5): Compound **4** (0.25 g, 0.7 mmol) was dissolved in dry CH₂Cl₂ (20 mL) under a nitrogen atmosphere. The temperature of the solution was lowered with an ice bath and excess HBr·AcOH (110 mL, 33%) was slowly added. The mixture was then stirred at room temperature for 15 h and then cooled to 0 °C. Subsequently, aqueous 6 M K₂CO₃ was slowly added until the solution reached a pH of 8. The organic layer was then collected, washed with water and brine, dried with MgSO₄, filtered and concentrated to ca. 5 mL. Addition of hexane caused the precipitation of **5** as a white crystalline material. The crystals were collected by filtration, washed with cold hexane and dried in

vacuo. Yield: 0.31 g, 64%. ¹H NMR (300 MHz, CDCl₃): δ = 8.75 [d, J_{H,H} = 4.8 Hz, 2 H, tpyH(6, 6'')], 8.73 [s, 2 H, tpy(3', 5')], 8.69 [d, J_{H,H} = 8.1 Hz, 2 H, tpy(3, 3'')], 7.90 [td, J_{H,H} = 7.80, 1.60 Hz, 2 H, tpy(4, 4'')], 7.85 (s, 2 H, ArH), 7.53 (s, 1 H, Ar), 7.38 [t, J_{H,H} = 6.13 Hz, 2 H, tpy(5, 5'')], 4.58 (s, 4 H, CH₂) ppm. ¹³C NMR (75 MHz, CDCl₃): δ = 156.3, 156.1, 149.3, 149.2, 139.9, 139.5, 137.2, 130.5, 128.1, 124.2, 121.7, 118.9, 32.7 (CH₂) ppm. Because of its toxicity, elemental and ESI analyses were not carried out. *Caution: Substituted benzyl bromides can be powerful lachrymators and should be used with adequate ventilation and precaution against skin contact or ingestion.*

4'-[C₆H₃{CH₂P(BH₃)Ph₂]₂-3,5]-2,2':6',2''-terpyridine ([tpyPC(H)P]-2BH₃, 6): *n*BuLi (0.8 mL, 1.34 mmol) was added to HPPH₂-BH₃ (0.27 g, 1.34 mmol) in dry THF (30 mL) at -78 °C. The temperature was allowed to rise to room temperature and stirring was continued overnight. A solution of **5** (0.32 g, 0.67 mmol) in dry THF (20 mL) was then added at -78 °C. The mixture was warmed to room temperature and stirred for ca. 20 h. All volatiles were then removed in vacuo, and the obtained residue was dissolved in CH₂Cl₂. The organic layer was washed with water and brine and dried with MgSO₄. Product **6** was obtained after evaporation of CH₂Cl₂ as a white solid that was washed with hot EtOH and hexane and dried in vacuo. Yield: 0.63 g, 64%. ¹H NMR (300 MHz, CDCl₃): δ = 8.77 [d, J_{H,H} = 4.0 Hz, 2 H, tpyH(6, 6'')], 8.60 [d, J_{H,H} = 7.8 Hz, 2 H, tpyH(3, 3'')], 8.19 [s, 2 H, PyrH(3', 5')], 7.86 [td, J_{H,H} = 7.8, 1.6 Hz, 2 H, tpyH(4, 4'')], 7.63 (m, 8 H, meta-H PAr), 7.47 (m, 12 H, ortho- and para-H PAr), 7.35 [t, J_{H,H} = 6.13 Hz, 2 H, tpyH(5, 5'')], 7.15 (s, 2 H, ArH), 6.95 (s, 1 H, Ar), 3.58 (d, ²J_{H,P} = 11.0 Hz, 4 H, CH₂), 0.90 (br. m, 6 H, BH₃) ppm. ¹³C NMR (75 MHz, CDCl₃): δ = 156.3, 155.9, 149.8, 149.0, 138.3, 137.2, 133.3, 132.9 (d, ¹J_{C,P} = 8.5 Hz, C_{quat}, PAr), 131.7, 129.0 (d, ²J_{C,P} = 9.2 Hz, PAr), 128.2, 128.0, 124.0, 121.7, 119.2, 34.2 (d, ¹J_{C,P} = 31.7 Hz, CH₂) ppm. ³¹P{¹H} NMR: δ = (121.4 MHz, CDCl₃): δ = 19.3 (br. m) ppm. C₃₅H₃₃B₂N₃P (548.25): calcd. C 76.97, H 5.91, N 5.73, B 2.95, P 8.45; found C 76.78, H 6.10, N 5.59, B 3.01, P 8.50.

4'-[C₆H₃(CH₂PPh₂)₂-3,5]-2,2':6',2''-terpyridine ([tpyPC(H)P], 7): Freshly distilled Et₃NH (5 mL) was added to a solution of **6** in CH₂Cl₂. The mixture was stirred at reflux for 4 h. All the volatiles were removed in vacuo, and the obtained white solid was redissolved in dry CH₂Cl₂ (10 mL). The organic layer was collected, washed with degassed water and brine and dried with MgSO₄. After evaporation of the CH₂Cl₂ in vacuo, product **7** was obtained as an extremely air- and moisture-sensitive white sticky solid. This product was used without further purification. Yield: 0.54 g, 88%. ¹H NMR (300 MHz, CDCl₃): δ = 8.76 [d, J_{H,H} = 3.0 Hz, 2 H, tpyH(6, 6'')], 8.75 [d, J_{H,H} = 3.0 Hz, 2 H, tpyH(3, 3'')], 8.38 [s, 2 H, tpyH(3', 5')], 7.86 [td, J_{H,H} = 7.5, 1.6 Hz, 2 H, tpyH(4, 4'')], 7.37 [m, 2 H, tpyH(5, 5'') and PAr], 7.18 (s, 2 H, ArH), 6.93 (s, 1 H, Ar), 3.39 (s, 4 H, CH₂) ppm. ¹³C NMR (75 MHz, CDCl₃): δ = 156.6, 155.9, 150.6, 149.2, 138.3, 138.2, 136.9, 133.2 (d, ¹J_{C,P} = 18.0 Hz, C_{quat}, PAr), 131.2, 129.0, 128.6 (d, ²J_{C,P} = 6.0 Hz, PAr), 126.4, 123.9, 121.6, 119.2, 36.2 (d, ¹J_{C,P} = 16.0 Hz, CH₂) ppm. ³¹P{¹H} NMR (121.4 MHz, CDCl₃): δ = -8.5 (s) ppm.

[Fe(tpy){tpyPC(H)P}](PF₆)₂ (9): Ligand **7** (0.17 g, 0.25 mmol) and [Fe(tpy)Cl₃] (0.095 g, 0.25 mmol) were heated at reflux in dry MeOH for 4 h. The yellow mixture rapidly turned purple upon heating. The solution was then cooled down to room temperature, filtered and excess NH₄PF₆ in degassed water was added. The formed deep purple precipitate was filtered off, washed with degassed water and dried in vacuo. Yield: 0.10 g, 40%. Removal of a small amount of a tpy-containing impurity by chromatography

could not be carried out because of the high sensitivity to air and moisture of the PPh₂ moieties. Complex **9** was used in the next reaction without further purification. ¹H NMR (300 MHz, CD₃CN): δ = 8.96 [d, J_{H,H} = 7.8 Hz, 2 H, tpyA(3', 5')], 8.70 [t, J_{H,H} = 8.1 Hz, 1 H, tpyA(4')], 8.51 [d, J_{H,H} = 8.4 Hz, 4 H, tpyA(3, 3'') + tpyA(3, 3'')], 7.98 [s, 2 H, tpyB(3', 5')], 7.91–7.86 [m, 4 H, tpyA(4, 4'') + tpyA(4, 4'')], 7.71 [d, J_{H,H} = 7.8 Hz, 2 H, tpyA(6, 6'')], 7.61 [d, J_{H,H} = 8.0 Hz, 2 H, tpyB(6, 6'')], 7.43–7.39 [m, 12 H, *para*-H + *meta*-H PAR], 7.34–7.28 [m, 6 H, Ar + tpyA(5, 5'') + tpyA(5, 5'')], 7.09 (m, 9 H, Ar + *ortho*-H PAR), 2.7 (s, 4 H, CH₂) ppm. ³¹P{¹H} NMR (121.4 MHz, CD₃CN): δ = -4.9 (s, 2 P), -143.28 (sept, ¹J_{P,F} = 705 Hz, [PF₆]⁻) ppm. ESI-MS: *m/z* = 497.20 [M - 2 PF₆]²⁺.

[Fe(tpy)(tpyPCP)Ru(tpy)](PF₆)₃ (**11**): Compounds **8** (0.10 g, 0.08 mmol) and **9** (0.05 g, 0.08 mmol) were dissolved in THF/MeCN (2:1, 30 mL). The solution was stirred at reflux for 10 h. The solvent was evaporated in vacuo. The deep purple residue was washed several times with hexane until no more free bis(amino)arene (NCN) ligand could be detected by ¹H NMR spectroscopy, and then dried in vacuo. The obtained deep purple solid (**10**), characterized only by NMR spectroscopy, was added to 2,2':6',2''-terpyridine (0.02 g, 0.08 mmol) dissolved in dry MeOH (25 mL). The mixture was heated at reflux for 2 d. Subsequently, the methanolic solution was cooled to room temperature, filtered, and concentrated until a small residual amount remained. Addition of aqueous NH₄PF₆ resulted in the precipitation of **11** as an air-stable red-purple solid that was collected by filtration, washed with water, hexane and dried in vacuo. The crude product was purified by column chromatography on silica gel (MeCN/water/saturated NaNO₃ solution 70:25:5). The major fraction was dried to afford **11** as a red-purple solid. Yield: 0.07 g, 52%. ¹H NMR (300 MHz, CD₃COCD₃): δ = 9.07 [d, J_{H,H} = 8.1 Hz, 2 H, tpyC(3', 5')], 8.86 [d, J_{H,H} = 8.1 Hz, 2 H, tpyA(3', 5')], 8.82–8.70 [m, 3 H, tpyA(4') + tpyC(3, 3'')], 8.58 [t, J_{H,H} = 8.5 Hz, 1 H, tpyC(4')], 8.48 [d, J_{H,H} = 8.1 Hz, 4 H, tpyA(3, 3'') + tpyB(3, 3'')], 8.09 [s, 2 H, tpyB(3', 5'')], 8.06–8.00 [m, 8 H, Ar + tpyA(4, 4'') + tpyB(4, 4'') + tpyC(4, 4'')], 7.69 [d, J_{H,H} = 5.4 Hz, 2 H, tpyC(6, 6'')], 7.42 [d, J_{H,H} = 5.1 Hz, 4 H, tpyA(6, 6'') + tpyA(6, 6'')], 7.64–7.53 [m, 6 H, tpyA(5, 5'') + tpyB(5, 5'') + tpyC(5, 5'')], 7.35–6.77 (m, 20 H, PAR) ppm. ³¹P{¹H} NMR (121.4 MHz, CD₃CN): δ = 41.82 (s, 2 P), -142.92 (sept, ¹J_{P,F} = 705 Hz, [PF₆]⁻) ppm. ESI-MS: *m/z* = 442.75 [M - 3 PF₆]³⁺, 736.67 [M - 2 PF₆]²⁺.

Acknowledgments

This work was financially supported by the Council for Chemical Sciences of the Netherlands Organization of Scientific Research (CW-NWO).

- [1] a) E. C. Constable in *Electronic Materials: The Oligomer Approach*, Wiley-VCH, Weinheim, **1998**; b) J.-P. Collin, P. Graña, V. Heitz, J.-P. Sauvage, *Eur. J. Inorg. Chem.* **1998**, 1–14; c) E. A. Harriman, R. Ziessel, *Coord. Chem. Rev.* **1998**, *171*, 331–339; d) R.-A. Fallahpour, *Synthesis* **2003**, 155–184; e) H. Hofmeier, U. S. Schubert, *Coord. Chem. Rev.* **2004**, *33*, 373–399; f) R. T. F. Jukes, V. Adamo, F. Hartl, P. Belser, L. De Cola, *Coord. Chem. Rev.* **2005**, *249*, 1327–1335.
- [2] a) E. C. Constable, A. M. W. Cargill Thompson, P. Harverson, L. Macko, M. Zehnder, *Chem. Eur. J.* **1995**, *1*, 360–367; b) S. Serroni, S. Campagna, F. Puntoriero, C. Di Pietro, N. D. McClenaghan, F. Loiseau, *Chem. Soc. Rev.* **2001**, *30*, 367–375.
- [3] a) B. G. G. Lohmeijer, U. S. Schubert, *Angew. Chem. Int. Ed.* **2002**, *41*, 3825–3829; b) B. G. G. Lohmeijer, U. S. Schubert, *J. Polym. Sci., Part A: Polym. Chem.* **2003**, *41*, 1413–1427; c) H.

- Hofmeier, A. El-Ghayoury, A. P. H. J. Schenning, U. S. Schubert, *Chem. Commun.* **2004**, *3*, 318–319.
- [4] V. W.-W. Yam, W. W. Lee, K. K. Cheung, *Organometallics* **1997**, *16*, 2833–2841.
- [5] E. A. Medlycott, G. S. Hannan, *Chem. Soc. Rev.* **2005**, *34*, 133–142.
- [6] M. Gagliardo, G. Rodriguez, H. H. Dam, M. Lutz, A. L. Spek, R. W. A. Havenith, P. Coppo, L. De Cola, F. Hartl, G. P. M. van Klink, G. van Koten, *Inorg. Chem.* **2006**, *45*, 2143–2155.
- [7] a) B. R. Steele, K. Vrieze, *Transition Met. Chem.* **1977**, *2*, 140–144; b) D. M. Grove, G. van Koten, H. J. C. Ubbels, R. Zoet, A. L. Spek, *Organometallics* **1984**, *3*, 1003–1009; c) J. A. M. van Beek, G. van Koten, M. J. Ramp, N. C. Coenjaarts, D. M. Grove, K. Goubiltz, M. C. Zoutberg, C. H. Stam, W. J. J. Smeets, A. L. Spek, *Inorg. Chem.* **1991**, *30*, 3059–3068; d) A. J. Canty, J. Patel, B. W. Skelton, A. H. White, *J. Organomet. Chem.* **2000**, *607*, 194–202; e) G. Rodríguez, M. Albrecht, J. Schoenmaker, A. Ford, M. Lutz, A. L. Spek, G. van Koten, *J. Am. Chem. Soc.* **2002**, *124*, 5127–5138.
- [8] H. P. Dijkstra, P. Steenwinkel, D. M. Grove, M. Lutz, A. L. Spek, G. van Koten, *Angew. Chem. Int. Ed.* **1999**, *38*, 2186–2188.
- [9] Representative examples of aryl pincer complexes applied as liquid crystalline materials, optical and electro-optical devices, sensors and catalysts: a) B. Donnio, D. W. Bruce in *Structure and Bonding (Liquid Crystals II)* (Ed.: D. M. P. Mingos), Springer, **1999**; b) M. Ghedini, G. Pucci, A. Crispini, I. Aiello, F. Barigelletti, A. Gessi, O. Francescangeli, *Appl. Organomet. Chem.* **1999**, *13*, 565–581; c) P. Espinet, E. Garcia-Orodea, J. A. Miguel, *Inorg. Chem.* **2000**, *39*, 3645–3651; d) L. Omnes, B. A. Timini, T. Gelbrich, M. B. Hursthouse, G. R. Luckhurst, D. W. Bruce, *Chem. Commun.* **2001**, 2248–2249; e) M. Albrecht, G. van Koten, *Angew. Chem. Int. Ed.* **2001**, *40*, 3750–3781; f) I. Aiello, D. Dattilo, M. Ghedini, A. Bruno, R. Termine, A. Golemme, *Adv. Mater.* **2002**, *14*, 1233–1236; g) M. Talarico, G. Barberio, D. Pucci, M. Ghedini, A. Golemme, *Adv. Mater.* **2003**, *15*, 1374–1377; h) M. E. van der Boom, D. Milstein, *Chem. Rev.* **2003**, *103*, 1759–1792; i) J. T. Singleton, *Tetrahedron* **2003**, *59*, 1837–1857; j) J. K. Szabó, *Synlett* **2006**, 811–824.
- [10] a) C. Moulton, B. L. Shaw, *J. Chem. Soc., Dalton Trans.* **1976**, 1020–1024; b) F. Gorla, L. M. Venanzi, A. Albinati, *Organometallics* **1994**, *13*, 43–54; c) A. Weisman, M. Gozin, H.-B. Kraatz, D. Milstein, *Inorg. Chem.* **1996**, *35*, 1792–1797; d) G. Jia, H. M. Lee, I. D. Williams, *J. Organomet. Chem.* **1997**, *534*, 173–180; e) M. E. van der Boom, S.-Y. Liou, Y. Ben-David, L. J. W. Shimon, D. Milstein, *J. Am. Chem. Soc.* **1998**, *120*, 6531–6541; f) M. E. van der Boom, H.-B. Kraatz, L. Hassner, Y. Ben-David, D. Milstein, *Organometallics* **1999**, *18*, 3873–3884; g) P. Dani, M. Albrecht, G. P. M. van Klink, G. van Koten, *Organometallics* **2000**, *19*, 4468–4476; h) D. G. Gusev, M. Madott, F. M. Dolgushin, K. A. Lyssenko, M. Y. Antipin, *Organometallics* **2000**, *19*, 1734–1739; i) R. M. Gauvin, H. Rozenberg, L. J. W. Shimon, D. Milstein, *Organometallics* **2001**, *20*, 1719–1724; j) M. W. Haenel, S. Oevers, K. Angermund, W. C. Kaska, H.-J. Fan, M. B. Hall, *Angew. Chem. Int. Ed.* **2001**, *40*, 3596–3600; k) D. Morales-Morales, R. E. Cramer, C. M. Jensen, *J. Organomet. Chem.* **2002**, *654*, 44–50.
- [11] a) P. Steenwinkel, S. L. James, D. M. Grove, N. Veldman, A. L. Spek, G. van Koten, *Chem. Eur. J.* **1996**, *2*, 1440–1445; b) A. Pape, M. Lutz, G. Müller, *Angew. Chem.* **1994**, *106*, 2375–2377; c) P. Steenwinkel, H. Kooijman, W. J. J. Smeets, A. L. Spek, D. M. Grove, G. van Koten, *Organometallics* **1998**, *17*, 5411–5426; d) M. Mehring, M. Schürmann, K. Jurkschat, *Organometallics* **1998**, *17*, 1227–1236; e) M. Albrecht, B. M. Kocks, A. L. Spek, G. van Koten, *J. Organomet. Chem.* **2001**, *624*, 271–286; f) H. P. Dijkstra, M. Q. Slagt, A. McDonald, C. A. Kruithof, R. Kreiter, A. M. Mills, M. Lutz, A. L. Spek, W. Klopffer, G. P. M. van Klink, G. van Koten, *Eur. J. Inorg. Chem.* **2003**, 830–838.

- [12] a) P. Dani, T. Karlen, R. A. Gossage, W. J. J. Smeets, A. L. Spek, G. van Koten, *J. Am. Chem. Soc.* **1997**, *119*, 11317–11318; b) M. Albrecht, P. Dani, M. Lutz, A. L. Spek, G. van Koten, *J. Am. Chem. Soc.* **2000**, *122*, 11822–11833.
- [13] a) E. C. Constable, G. Baum, E. Bill, R. Dyson, R. van Eldik, D. Fenske, S. Kaderli, D. Morris, A. Neubrand, M. Neuburger, D. R. Smith, K. Wieghardt, M. Zehnder, A. D. Zuberbühler, *Chem. Eur. J.* **1999**, *5*, 498–508; b) P. S. Braterman, J.-L. Song, R. D. Peacock, *Inorg. Chem.* **1992**, *31*, 555–559; c) X. Zhou, A.-M. Ren, J.-K. Feng, *J. Organomet. Chem.* **2005**, *690*, 338–347.
- [14] M. Gagliardo, H. P. Dijkstra, P. Coppo, L. De Cola, M. Lutz, A. L. Spek, G. P. M. van Klink, G. van Koten, *Organometallics* **2004**, *23*, 5833–5840.
- [15] H. P. Dijkstra, M. D. Meijer, J. Patel, R. Kreiter, G. P. M. van Klink, M. Lutz, A. L. Spek, A. J. Canty, G. van Koten, *Organometallics* **2001**, *20*, 3159–3168.
- [16] a) J. K. Stille, *Pure Appl. Chem.* **1985**, *57*, 1171–1780; b) M. Heller, U. S. Schubert, *J. Org. Chem.* **2002**, *67*, 8269–8272.
- [17] K. T. Potts, D. Konwar, *J. Org. Chem.* **1991**, *56*, 4815–4816.
- [18] K.-H. Duchêne, F. Vögtle, *Synthesis* **1986**, 659–661.
- [19] a) E. C. Constable, C. E. Housecroft, M. Neuburger, A. G. Schneider, M. Zehnder, *J. Chem. Soc., Dalton Trans.* **1997**, 2427–2434; b) E. C. Constable, C. E. Housecroft, A. G. Schneider, *J. Organomet. Chem.* **1999**, *573*, 101–108; c) E. C. Constable, C. E. Housecroft, M. Neuburger, A. G. Schneider, B. Springler, M. Zehnder, *Inorg. Chim. Acta* **2000**, *300–302*, 49–55.
- [20] H. P. Dijkstra, M. Albrecht, G. van Koten, *Chem. Commun.* **2002**, 126–127.
- [21] J.-P. Sutter, S. L. James, P. Steenwinkel, T. Karlen, D. M. Grove, N. Veldman, W. J. J. Smeets, A. L. Spek, G. van Koten, *Organometallics* **1996**, *15*, 941–948.
- [22] D. J. Hathcock, K. Stone, J. Madden, S. J. Slattery, *Inorg. Chim. Acta* **1998**, *282*, 131–135.
- [23] J.-P. Sauvage, J.-P. Collin, J.-C. Chambron, S. Guillerez, C. Coudret, V. Balzani, F. Barigelletti, L. De Cola, L. Flamigni, *Chem. Rev.* **1994**, *94*, 993–1019.
- [24] a) P. Lainé, F. Bedioui, P. Ochsenbein, V. Marvaud, M. Bonin, E. Amouyal, *J. Am. Chem. Soc.* **2002**, *124*, 1364–1377.
- [25] a) M. Krejčík, M. Daněk, M. F. Hartl, *J. Electroanal. Chem. Interfacial Electrochem.* **1991**, *317*, 179–187; b) F. Hartl, H. Luyten, H. A. Nieuwenhuis, G. C. Schoemaker, *Appl. Spectrosc.* **1994**, *48*, 1522–1528.
- [26] S. Barlow, D. O'Hare, *Chem. Rev.* **1997**, *97*, 637–669.
- [27] V. V. Pavlishchuk, A. W. Addison, *Inorg. Chim. Acta* **2002**, *298*, 97–102.
- [28] G. Gritzner, J. Kůta, *Pure Appl. Chem.* **1984**, *56*, 461–466.

Received: October 2, 2006

Published Online: February 14, 2007